Generalized Circuit Representation for a Synchronous Machine

Zhixin Miao, Senior Member, IEEE, Lingling Fan, Fellow, IEEE

Abstract—In this letter, a generalized circuit representation for a synchronous machine is presented. This circuit represents voltage and current relationship and can be used for dynamic and harmonic analysis. A distinct feature of the circuit is the use of Laplace transform variable s, which simplifies both calculus and frame conversion. Two derivation approaches are presented. The first approach starts from a steady-state circuit representation, while the second approach starts from the dq-frame dynamic model of a synchronous generator. Both arrive at the same representation.

Index Terms—Synchronous machines, dynamics, harmonics, circuit representation

I. INTRODUCTION

TEINMETZ developed the steady-state induction machine circuit representation in the early 20th century. This circuit concisely describes the relationship among the stator/rotor voltage/current phasors and has been presented in classic machine textbooks. Based on this circuit, the authors have derived the generalized circuit for induction machines which is applicable of dynamic analysis [1]. The same circuit representation was also found by use of the dq frame dynamic model with flux linkages as state variables in [2].

In this letter, we further examine the generalized dynamic circuit representation of a synchronous machine. Compared to an induction machine, a synchronous machine can be viewed as an induction machine with unbalanced rotor conditions. During the starting process, a synchronous machine's stator circuit currents have not only fundamental components but also harmonic components. The frequency of the harmonics depends on the rotating speed.

In majority of the textbooks, a steady-state circuit representation of a round rotor synchronous generator is simply a Thévinin equivalent: a voltage source behind a synchronizing reactance. This equivalent circuit assumes that the machine is operating at the synchronous speed. Thus, slip representation no longer exists. However, a diligent search by the authors leads to the finding of a less known steady-state circuit representation of a synchronous machine that is applicable at any rotating speed. In 1950s, Garbarino and Gross examined induction machines with unbalanced rotor conditions and presented several circuit representations [3].

In this letter, this circuit will be further extended to a generalized dynamic circuit for a synchronous machine. A second derivation approach is also presented. This approach starts from the dynamic model. It can be seen that both arrive at the same circuit representation. Using this circuit representation, for a given stator voltage and a given speed,

This project is supported in part by US NSF award 2103480 and in part by US DOE DE-EE-0008771. L. Fan and Z. Miao are with the Department of Electrical Engineering, University of South Florida, Tampa, FL, 33620 (e-mail: linglingfan, zmiao@usf.edu).

the sequence/harmonic components of the stator and field currents can be found. In turn, the harmonic components of the electromagnetic torque can be computed. Combined with the swing dynamics, a first-order phasor-based dynamic model is developed to simulate the staring process of a synchronous machine. The simulation results have been compared with those generated from an electromagnetic transient (EMT) testbed. Comparison shows that the proposed circuit leads to accurate torque and current computing results. The circuit is useful for both dynamic analysis and harmonic analysis.

II. APPROACH 1

A round rotor synchronous machine without the dc excitation voltage source can be viewed as an inductor machine with its rotor circuits' two phases short circuited, while another left open. The rotor's terminal voltages and the currents have the following relationship:

$$\overline{V}_{r,bn} = \overline{V}_{r,cn}, \ \overline{I}_{ra} + \overline{I}_{rb} = 0, \ \overline{I}_{rc} = 0.$$
 (1)

Applying the symmetrical component transform leads to the following relationship for the sequence voltage and current components.

$$\overline{V}_{r}^{+} = \overline{V}_{r}^{-}, \ \overline{I}_{r}^{+} + \overline{I}_{r}^{-} = 0.$$
 (2)

Thus, the positive- and the negative- sequence circuits are interconnected at the rotor terminal as two parallel circuits. This network representation is based on the view point of the rotor. Hence, the perturbing frequency is the slip frequency notated as ω_r . To view the circuit from the stator side, we may conduct impedance scaling and voltage scaling. Fig. 1 presents the network viewed from the stator. This network representation can be found in the 1950 paper by Garbarino and Gross [3] (Fig. 3). A more detailed step-by-step derivation procedure can be found in the authors' work [4].

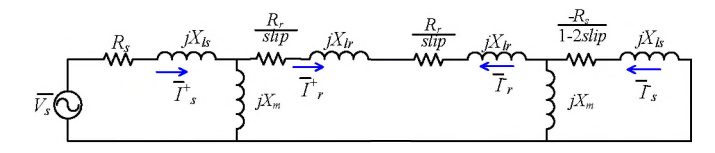


Fig. 1: The sequence network of an induction machine with its rotor circuits phase b and phase c short circuited while phase a left open.

This steady-state circuit is viewed from the stator's side when the perturbing frequency is ω_s , the synchronous frequency. Thus, replacing $j\omega_s$ by s in the reactance representation, and replacing the slip by $\frac{s-j\omega_m}{s}$, where ω_m is the rotor speed, we may quickly arrive at the dynamic circuit representation. If we notate the rotor resistance and inductance as a synchronous machine's field resistance R_f and leakage

inductance \mathcal{L}_{lf} , the final representation is shown in Fig. 3 in Section III.

This derivation philosophy is to treat the steady-state circuit representation as a special case of the generalized dynamic circuit when the stator side's perturbation frequency is ω_s . On the other hand, in the dynamic circuit, $j\omega_s$ can all be replaced by the Laplace transform variable s. Hence, the stator leakage reactance, the rotor leakage reactance and the magnetizing reactance, such as $j\omega_s L_{ls}$, $j\omega_s L_{lf}$ and $j\omega_s L_m$ can be expressed as sL_{ls} , sL_{lf} and sL_m . In the steady-state circuit, the equivalent rotor resistance R_r/slip is tricky to be converted to a dynamic impedance. A close examination of the slip leads to the following discovery [1].

$$\mathrm{slip} = 1 - \frac{\omega_m}{\omega_s} = 1 - \frac{j\omega_m}{j\omega_s}, \Longrightarrow \mathrm{slip}(s) = 1 - \frac{j\omega_m}{s}.$$

Hence,
$$\frac{2R_r}{\text{slip}} = \frac{s}{s - j\omega_m} 2R_r$$
, $\frac{-R_s}{1 - 2\text{slip}} = \frac{s}{s - j2\omega_m} R_s$.

Thus, a steady-state circuit representation can be converted to a generalized dynamic circuit.

III. APPROACH 2

We now examine a synchronous generator with an excitation circuit. The dynamic model in time domain is presented as follows. First, the relationship of the stator voltages, the stator currents, and the stator flux is expressed in (3).

$$v_d = -i_d R_s - \omega_m \lambda_q + \dot{\lambda_d}, \ v_q = -i_q R_s + \omega_m \lambda_d + \dot{\lambda_q} \ \ (3)$$

where the flux linkages are related to the dq stator current and the excitation current i_{fd} as follows.

$$\lambda_d = (L_{md} + L_{ls})(-i_d) + L_{md}i_{fd},$$

$$\lambda_q = (L_{mq} + L_{ls})(-i_q)$$
(4)

Next, for the rotor excitation circuit, the voltage and current relationship is:.

$$v_{fd} = i_{fd}R_f + \dot{\lambda_{fd}}, \tag{5}$$

where $\lambda_{fd} = L_{md}(-i_d) + (L_{md} + L_{lf})i_{fd}$.

For generalized circuit representation, we aim to present the voltage and current relationship explicitly. The dynamic model ((3) and (5)) do not meet the requirement since the speed voltage terms is related to the flux linkages. To get rid of the speed voltages, we seek to use complex vector in the Laplace domain. From (3), it can be found that

$$V_1(s) = -R_s I_1(s) + (s + j\omega_m) \Lambda_1(s)$$
 (6)

$$V_2(s) = -R_s I_2(s) + (s - j\omega_m) \Lambda_2(s) \tag{7}$$

where $F_1(s) = f_d(s) + jf_q(s)$, $F_2(s) = f_d(s) - jf_q(s)$, with F being the complex vector V, I or Λ , and f being v, i, or λ .

A. Physical meaning of the complex vectors $F_1(s)$ and $F_2(s)$

Harnefors initiated the use of complex vector in the analysis of dq-frame converter control [5] and this concept has been used extensively in the literature of power electronics control. Among them, asymmetrical-dynamics-induced mirror frequency has been discussed in [6], [7]. In this letter, the prime and mirror frequency components will be expressed more concisely using the Laplace transform variable s.

Suppose that the dq-frame currents $i_d(t)$ and $i_q(t)$ viewed from the rotor are sinusoidal signals with a frequency of ω_r . The machine has a rotating speed of ω_m . The d-axis current i_d creates two space vectors, one at the frequency of $\omega_r + \omega_m = \omega_s$ and the other at the frequency of $-\omega_r + \omega_m = 2\omega_m - \omega_s$. Similarly, the q-axis current i_q also create two space vectors of the two frequencies. Hence, in the stator side, the stator current should have two harmonic components: the primary component at ω_s and the mirror frequency component at $2\omega_m - \omega_s$. Only if the two signals have the same magnitudes and i_q lags i_d by 90 degree, the two space vectors at the mirror frequency are canceled by each other with the stator currents having only ω_s component.

The space vector formed by the three-phase currents (notated as $\vec{i}(t)$) has the following relationship with $i_d(t)$ and $i_q(t)$: $\vec{i}(t) = (i_d(t) + ji_q(t))e^{j\omega_m t}$. Notate the analytic form of $i_d(t)$ as $\tilde{i}_d(t)$ and the analytical form of $i_q(t)$ as $\tilde{i}_q(t)$. Then the space vector $\vec{i}(t)$ can be written as:

$$\vec{i}(t) = \left(\underbrace{\frac{1}{2}\left(\tilde{i}_d(t) + j\tilde{i}_q(t)\right)}_{I_1(t)} + \underbrace{\frac{1}{2}\left(\tilde{i}_d^*(t) + j\tilde{i}_q^*(t)\right)}_{I_2^*(t)}\right) e^{j\omega_m t} \tag{8}$$

Note that $\tilde{i}_d(t)$, $\tilde{i}_q(t)$, and $I_1(t)$ are analytic signals with a frequency of ω_r , while $\tilde{i}_d^*(t)$, $\tilde{i}_q^*(t)$, and $I_2^*(t)$ are analytic signals with a frequency of $-\omega_r$. Both $I_1(t)$ and $I_2(t)$ are analytical signals with a frequency of ω_r . In the Laplace domain, it can be seen that

$$I_1(s) = i_d(s) + ji_q(s), \quad I_2(s) = i_d(s) - ji_q(s).$$
 (9)

Remark: Therefore, the complex vectors represent the primary frequency component and the conjugate of the mirror frequency component, viewed in the rotor frame.

Furthermore, the primary frequency component, notated as i_1 viewed from the stator frame has the following relationship with $I_1(s)$:

$$i_1(s+j\omega_m) = I_1(s)$$
, or $i_1(s) = I_1(s-j\omega_m)$.

The mirror-frequency component's conjugate, notated as i_2 has the following time-domain format $I_2(t)e^{-j\omega_m t}$. Hence, their Laplace-domain expressions are related as

$$I_2(s) = i_2(s - j\omega_m), \Longrightarrow I_2(s - j\omega_m) = i_2(s - j2\omega_m).$$

B. Generalized circuit development

For simplicity, round rotor structure is assumed and the dq-axis inductances are the same: $L_{md} = L_{mq} = L_m$. The flux linkages and the currents have the following relationship.

$$\begin{bmatrix} \Lambda_1 \\ \Lambda_2 \end{bmatrix} = \begin{bmatrix} L_m + L_{ls} & 0 \\ 0 & L_m + L_{ls} \end{bmatrix} \begin{bmatrix} -I_1 \\ -I_2 \end{bmatrix} + \begin{bmatrix} L_m \\ L_m \end{bmatrix} i_{fd} \quad (10)$$

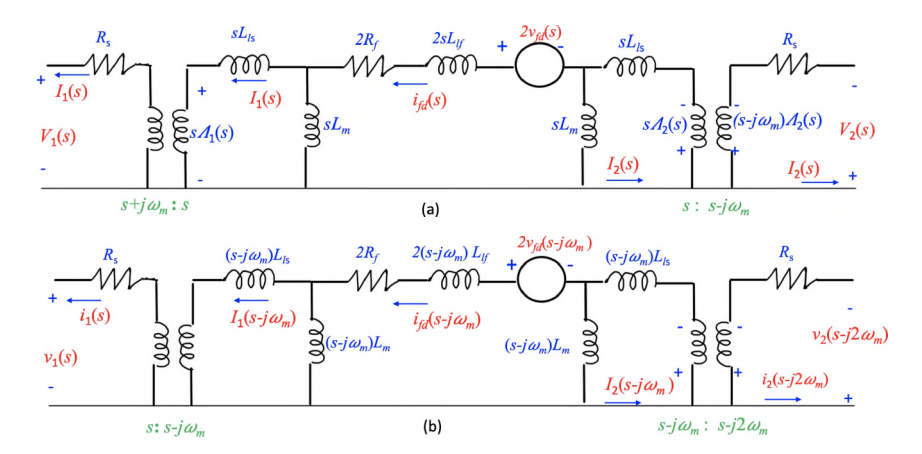


Fig. 2: Circuit representation of a round rotor synchronous machine. (a) Step 1. (b) Step 2.

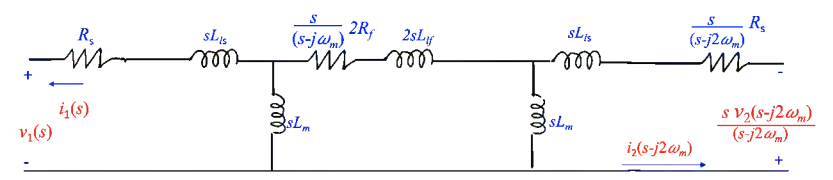


Fig. 3: Circuit representation of a round rotor synchronous machine without excitation voltage source.

It can be seen that the excitation current contributes to both flux linkage complex vectors. On the other hand, (5) is still expressed by the d-axis flux linkage λ_{fd} . We will express λ_{fd} by use of the complex vectors of the current.

$$\lambda_{fd} = L_m \left(\frac{-I_1}{2} + \frac{-I_2}{2} \right) + (L_m + L_{lf})i_{fd}, \quad (11)$$

$$\implies 2\lambda_{fd} = L_m (-I_1 - I_2) + 2(L_m + L_{lf})i_{fd}.$$
 (12)

Thus, the flux linkage linked with the excitation circuit has contributions from the two current complex vectors and the excitation current.

Based on the above relationship, we may construct a circuit representing the formation of the three flux linkages first: stator flux linkage's complex vectors and the rotor excitation field flux linkage λ_{fd} . The circuit is shown in Fig. 2(a), where both $-I_1$ and i_{fd} contribute to Λ_1 , and both $-I_2$ and i_{fd} contribute to Λ_2 .

Since the induced voltage from Λ_1 is $s\Lambda_1$, it has to be amplified to $\frac{s+j\omega_m}{s}$ times to be connected to $V_1(s)$ through the resistor R_s . Similarly, the induced voltage from Λ_2 is $s\Lambda_2$. This voltage has to be amplified by $\frac{s-j\omega_m}{s}$ times to be connected to $V_2(s)$. Two transformer like symbols are used to represent the amplification. These two symbols represent voltage changes from one side to another. The currents at the two sides keep the same.

In step 2, the input voltage is viewed from the stator and notated as $v_1(s)$. Note that $v_1(s) = V_1(s-j\omega_m)$. We will replace s by $s-j\omega_m$ in Fig. 2(a). In turn, the previous circuit components viewed from the rotor frame have their s replaced by $s-j\omega_m$. For the rightmost part of the circuit, the terminal voltage and currents are $v_2(s-j2\omega_m)$ and $i_2(s-j2\omega_m)$.

In the last step, the two transformer like symbols are taken out. The excitation voltage v_{fd} is assumed to be 0. The middle part of the circuit between the two transformers has every impedance scaled by $\frac{s}{s-j\omega_m}$. This scaling effort makes sure

that the voltages at the two sides of the first transformer are now the same while the current is kept intact. For the rightmost part of the circuit, the scaling factor is $\frac{s}{s-j2\omega_m}$. The resulting circuit is Fig. 3. It can be seen that while all inductance has its impedance represented as sL, the rotor resistance and the stator resistance in the mirror-frequency domain are scaled by $\frac{s}{s-i\omega_m}$ and $\frac{s}{s-j2\omega_m}$.

If the perturbation frequency is the synchronous frequency ω_s , we may replace s by $j\omega_s$. The equivalent rotor resistance now becomes $\frac{2R_f}{\text{slip}}$ and the stator resistance in the mirror-frequency domain is $\frac{R_s}{2\text{slip}-1}$. We can see that the resulting steady-state circuit is the same as that in Fig. 1.

In short, a synchronous generator can be viewed as a twoport circuit connecting the primary frequency components with the mirror-frequency components.

IV. CASE STUDY: STARTING A SYNCHRONOUS MACHINE

The proposed circuit can be used to build a simulation model of starting a sychronous machine from standstill. Both the excitation voltage source v_{fd} and the mechanical torque T_m are set to 0. Based on the circuit in Fig. 3, at any given speed and for a given stator voltage, the stator current phasors and the field current phasors can be found by ignoring the EMT dynamics. Furthermore, the torque can be computed from these current phasors. The average torque is expressed as follows:

$$T_{\rm em,avg} = L_m {
m Imag} \left(i_1(s) [i_{fd}(s-j\omega_m)]^* + \\ + i_{fd}(s-j\omega_m) [i_2(s-j2\omega_m)]^* \right) \quad (13)$$

where s is evaluated at the nominal frequency of 377 rad/s.

During starting process, the torque has both a dc component and a harmonic component. Since we are interested in the dynamics of accelerating a machine, we may compute only the useful torque, i.e., the average torque, for electromechanical

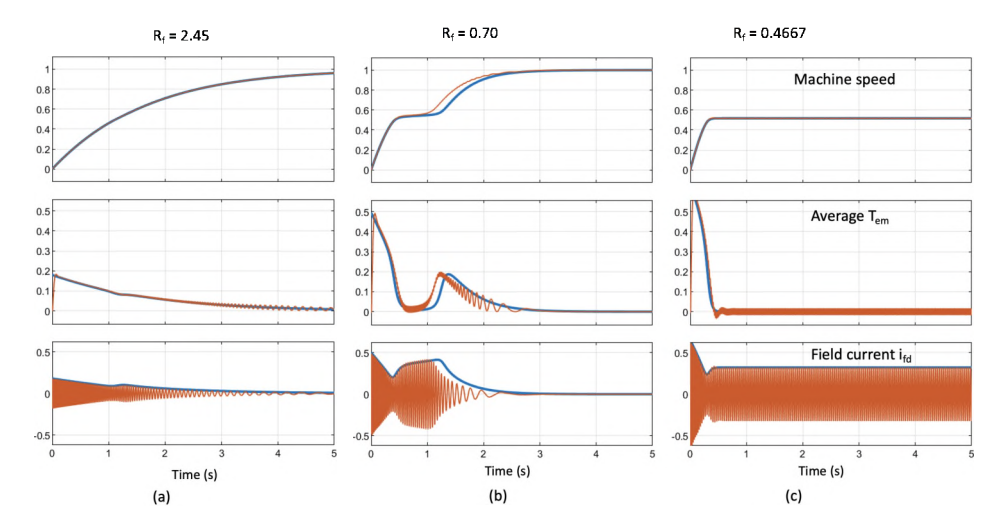


Fig. 4: Comparison of the simulation results of the phasor model (blue lines) and the EMT testbed (orange lines) for three scenarios of different field resistance. (1) Full speed is achieved. (2) The machine achieves full speed after staggering at half speed. (3) The machine achieves only half speed. The machine parameters in p.u.: stator resistor, leakage, dq mutual inductance and inertia: 0.2917, 0.0113, 3.0314, 3.0314, 0.1492; rotor resistance and leakage: 0.4667, 0.0490.

dynamics simulation. Combined with the circuit analysis and torque computing, the swing equation can be integrated and dynamic simulation results are produced based on this first-order model. For comparison, an EMT testbed with a generator model from the MATLAB/Simscape library is also built. The machine's d-axis has a field winding and a damping winding and its q-axis has two damping windings. Thus, the generator model contains both the first-order swing dynamics and the sixth-order electromagnetic dynamics. For a fair comparison, the impedances of three damping windings in the EMT model have been increased to large numbers.

Three cases are examined for a varying field resistance. When $R_f=2.45\,$ p.u., the machine can be accelerated from standstill to the full speed. When $R_f=0.7\,$ p.u., the machine can still be accelerated from standstill to the full speed. However, in between, it staggered at half of the full speed for a while. When $R_f=0.4667\,$ p.u., the machine can only be accelerated to 51% of the full speed. The last case demonstrates the Goerge's phenomenon [8].

Fig. 4 shows the simulation results. The phasor model has the machine speed, the average torque, and the field current's phasor's magnitude exported. From the EMT testbed, the measured torque has to be passed to a second-order low-pass filter first to have its dc component, or the average torque taken out. This filtered torque will be compared with the average torque from the phasor model. The measured field current from the EMT testbed is sinusoidal and with a varying frequency, while the phasor model exports the field current phasor's magnitude. These two are plotted together.

From the comparison of Fig. 4, we can see that even we ignored the electromagnetic dynamic in the phasor model, the phasor model with only first-order swing dynamics included can accurately capture the machine electromechanical behavior. In addition, the computed average torque and the field current phasor can also accurately reflect the true values in general.

In addition, harmonic analysis can be carried out using the circuit at two conditions: (i) at the beginning of the starting

process when the mechanical speed is still 0, and (ii) at the steady-state condition of Goerge's phenomenon when the machine's speed keeps at 0.51 p.u. The results from the phasor model have all been verified using the measurements from the EMT testbed. In summary, the circuit gives accurate harmonic component analysis results.

V. CONCLUSION

We present a generalized circuit representation for a synchronous machine suitable for dynamic and harmonic analysis. This representation takes the full advantage of the Laplace transform variable s in dealing with frame conversion and calculus. The resulting circuit representation of a synchronous machine is a two-port circuit connecting the stator's primary frequency components with the stator's mirror-frequency components. This circuit can also be viewed as a model representing the relationship of dynamic phasors of the primary frequency components and the mirror-frequency components.

REFERENCES

- [1] L. Fan and Z. Miao, "Nyquist-stability-criterion-based ssr explanation for type-3 wind generators," vol. 27, no. 3, pp. 807–809, 2012.
- [2] Z. Miao, "Impedance-model-based ssr analysis for type 3 wind generator and series-compensated network," *IEEE Transactions on Energy Conver*sion, vol. 27, no. 4, pp. 984–991, 2012.
- [3] H. L. Garbarino and E. T. Gross, "The goerges phenomenon-induction motors with unbalanced rotor impedances," *Transactions of the American Institute of Electrical Engineers*, vol. 69, no. 2, pp. 1569–1575, 1950.
- [4] R. Kar, Z. Miao, and L. Fan, "Circuit analysis of goerges phenomenon in a three-phase induction machine," in *IEEE Power & Energy Society General Meeting (PESGM)*, 2022, pp. 1–5.
- [5] L. Harnefors, "Modeling of three-phase dynamic systems using complex transfer functions and transfer matrices," *IEEE Transactions on Industrial Electronics*, vol. 54, no. 4, pp. 2239–2248, 2007.
- [6] A. Rygg, M. Molinas, C. Zhang, and X. Cai, "A modified sequence-domain impedance definition and its equivalence to the dq-domain impedance definition for the stability analysis of ac power electronic systems," *IEEE Journal of Emerging and Selected Topics in Power Electronics*, vol. 4, no. 4, pp. 1383–1396, 2016.
- [7] X. Wang, L. Harnefors, and F. Blaabjerg, "Unified impedance model of grid-connected voltage-source converters," *IEEE Transactions on Power Electronics*, vol. 33, no. 2, pp. 1775–1787, 2017.
- [8] H. Görges, "über Drehstrommotoren mit verminderter Tourenzahl," Elektrotech. Z, vol. 17, p. 192, 1896.